Appl Magn Reson (2012) 43:289–297
DOI 10.1007/s00723-012-0348-3

Applied
Magnetic Resonance

Measurement of Arterial Input Function in Hyperpolarized ^{13}C Studies

Małgorzata Marjańska · Thomas Z. Teisseyre · Nicholas W. Halpern-Manners · Yi Zhang · Isabelle Iltis · Vikram Bajaj · Kamil Ugurbil · Alexander Pines · Pierre-Gilles Henry

Received: 10 February 2012 / Revised: 13 April 2012 / Published online: 20 May 2012

Abstract Recently, hyperpolarized substrates generated through dynamic nuclear polarization have been introduced to study in vivo metabolism. Injection of hyperpolarized [1-^{13}C] pyruvate, the most widely used substrate, allows detection of time courses of [1-^{13}C] pyruvate and its metabolic products, such as [1-^{13}C] lactate and ^{13}C-bicarbonate, in various organs. However, quantitative metabolic modeling of in vivo data to measure specific metabolic rates remains challenging without measuring the input function. In this study, we demonstrate that the input function of [1-^{13}C] pyruvate can be measured in vivo in the rat carotid artery using an implantable coil.

1 Introduction

Recently, hyperpolarized substrates generated through dynamic nuclear polarization (DNP) have been introduced to study in vivo metabolism [1]. [1-^{13}C] pyruvate has been the most widely used substrate for metabolic studies. [1-^{13}C] pyruvate metabolism to [1-^{13}C] lactate (via lactate dehydrogenase (LDH)), [1-^{13}C] alanine

M. Marjańska (✉) · Y. Zhang · I. Iltis · K. Ugurbil · P.-G. Henry
Department of Radiology and Center for Magnetic Resonance Research,
University of Minnesota, 2021 6th Street SE, Minneapolis, MN 55455, USA
e-mail: gosia@cmrr.umn.edu

T. Z. Teisseyre · N. W. Halpern-Manners · V. Bajaj · A. Pines
Department of Chemistry, University of California at Berkeley, Berkeley, CA 94720, USA

T. Z. Teisseyre
Joint Graduate Group in Bioengineering, UCSF and UC Berkeley, San Francisco, CA, USA

N. W. Halpern-Manners · V. Bajaj · A. Pines
Materials Sciences Division, E. O. Lawrence Berkeley National Laboratory,
Berkeley, CA 94720, USA

(via alanine aminotransferase), and ^{13}C bicarbonate (via pyruvate dehydrogenase complex (PDH) and carbonic anhydrase) has been observed in vivo using magnetic resonance techniques [2].

Altered metabolism in cancer has been detected using the lactate-to-pyruvate ratio at a single point in time [3–5]. This approach is very sensitive to the timing of the data acquisition, the injection of pyruvate, and the arrival of pyruvate to the tissue of interest. An alternative approach is to measure the lactate and pyruvate signals over time and fit these to a kinetic model [5–9]. However, these kinetic models are generally not measuring metabolic rates through specific enzymes or pathways. Rather, they measure apparent rates of label incorporation from a substrate to its metabolic product. Few attempts have been made to develop metabolic models to fit ^{13}C hyperpolarized data in vivo in order to determine actual metabolic rates [10, 11].

One limiting factor in such metabolic modeling of in vivo data is the difficulty to measure the input function, i.e., the time course of the injected ^{13}C-labeled substrate in the blood. Obtaining the input function directly from the measured ^{13}C metabolic images is impossible for hyperpolarized substrates due to low signal-to-noise ratio (SNR), absence of clearly visible artery, and the size of voxel used with magnetic resonance spectroscopic imaging.

In this study, we demonstrate the feasibility of measuring the arterial input function of [1-^{13}C] pyruvate in vivo in rat using an implantable coil around the carotid artery.

2 Materials and Methods

2.1 Implantable Coil

Implantable coils were designed in AUTOCAD (Autodesk, Inc., San Rafael, CA) (Fig. 1a) and fabricated on a flexible printed circuit board (PCB) using a proprietary low loss tangent substrate (CuFlon from Polyflon Co, Norwalk, CT). A CuFlon sheet was made of a double-sided layer of plated copper separated by a thin layer of

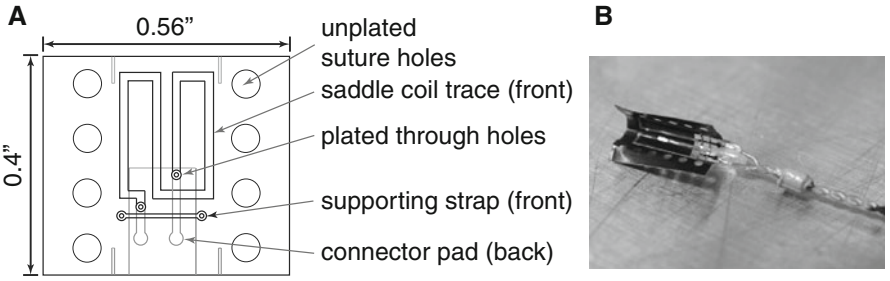

Fig. 1 Implantable radiofrequency coil. **a** Schematic of the coil. The *top layer* is outlined in *black* and the *bottom layer* is outlined in *gray*. **b** Picture of fully assembled coil with twisted pair of leads epoxied for support. Leads were then connected to a resonant circuit

polytetrafluoroethylene (PTFE). Each individual coil spanned the front and back layers of the sheet (Fig. 1a). Layers were electrically connected by plated through holes. Fabrication began with a ½ oz. (0.7 mils) sheet of CuFlon onto which the patterns were printed and through holes were drilled. The final sheet consisted of 1.5 oz. copper (2.1 mils) with 1 oz. in the through holes. All copper traces were finished with an immersion tin to help in soldering and to reduce board oxidation.

The entire body of the coil, including shielding, was 0.4 in. long and 0.58 in. wide. The actual printed coil (saddle coil with a supporting horizontal strap across the leads) on the top layer was 0.2 in. in length and 0.23 in. in width. Unplated through holes around the periphery of each individual coil were used to thread sutures during implantation to hold the coil in place around the blood vessel and maintain a cylindrical configuration during experiments. Plated through holes allowed for electrical contact between the layers, and led to the back side of the coil that contained the printed leads with contact pads that soldered to a twisted pair of braided lead wires (Fig. 1b). The twisted pair of lead wires connected the coil to a resonant circuit which allowed tuning the coil to 100 MHz. In addition to the leads and connector pads, a passive shield of copper covered the entire back side of the coil outside of the printed leads. The shield is contained outside of the rectangular segment surrounding the contact pads in Fig. 1a.

2.2 Hyperpolarized Samples

Aliquots ($\sim$10 μL) of the mixture of pure [1-^{13}C] pyruvic acid (Isotec, Miamisburg, OH) and 15 mM Tris{8-carboxyl-2,2,6,6-tetra(2-(1-hydroxyethyl))-benzo[1,2-d:4,5-d']bis(dithiole-2-yl)methyl} sodium salt (OX63 trityl radical) were placed into liquid helium and hyperpolarized by DNP (HyperSense, Oxford Instruments, UK) in a field strength of 3.35 T at approximately 1.4 K for 90 min (time constant $\sim$700 s). [1-^{13}C] pyruvate samples were then dissolved in 40 mM TRIS buffer, 40 mM NaOH and 0.32 mM Na_2EDTA solution to produce 4 mL of hyperpolarized solutions at a concentration of $\sim$35 mM and a pH of 7.

2.3 Animal Experiments

Three male Sprague–Dawley rats were used for the experiments: one animal was used for blood collection for in vitro measurements of T_1 of pyruvate and pyruvate hydrate in blood, one animal was used for collection of blood samples to measure concentration and enrichment of pyruvate, one animal was used for in vivo experiments with implantable neck coil. Three time courses were obtained in vivo after three injections of hyperpolarized mixture of pyruvate and pyruvate hydrate.

2.3.1 Collection of Blood Samples for In Vitro Experiments

A cannula was surgically placed in the femoral veins and arteries of a male Sprague–Dawley rat under isoflurane anesthesia. Blood was collected in 1 mL syringes and transferred to heparinized blood collection tubes. Approximately 11 mL of blood was collected. The samples were kept at room temperature and used

within 2 h of collection. Blood samples were discarded with biohazard disposal after use. Anesthesia depth was checked throughout the procedure. The animal was kept stable and warm throughout and euthanized after the procedure.

2.3.2 Concentration and Enrichment of ^{13}C-pyruvate in Blood

Cannulas were surgically placed in the femoral veins and arteries of a male Sprague–Dawley rat. Before injection of pyruvate, two blood samples (0.1 mL) were collected for baseline measurement. The time point of 0 reflects the average of these 2 collections before injection. After the injection of 2.3 mL of ^{13}C-pyruvate, 0.1 mL aliquots of blood were withdrawn every 10 s up to 90 s after the injection. Samples were centrifuged and plasma glucose concentration was measured immediately using a glucose analyzer (Analox Instruments, London, UK). Plasma samples were collected, freeze-dried and re-dissolved in D_2O. The concentration and enrichment ([^{13}C-pyr]/[pyr]) of ^{13}C-pyruvate were measured using high-resolution NMR spectroscopy (600 MHz) using glucose as an internal standard.

2.3.3 Animal Preparation for In Vivo Experiments

All animal experiments were performed in accordance with the National Institutes of Health *Guide for the Care and Use of Laboratory Animals* and were approved by the Institutional Animal Care and Use Committee of the University of Minnesota. One male Sprague–Dawley rats (285 g, Charles River Laboratories, Inc.) was used for this study. Anesthesia was induced with 5 % isoflurane, and rat was orally intubated and mechanically ventilated by 2 % isoflurane with 2:1 N_2O:O_2 mixture. The rat was placed in the supine position and the common carotid artery (CCA) was exposed through a midline neck incision. After CCA was carefully dissected free from surrounding nerves and fascia, the radiofrequency coil was placed around it and secured by suture to a natural position. In addition, femoral artery and vein were catheterized for physiological monitoring, blood sampling, and chemical administration. Upon completion of the surgical preparation, the incision was closed and the rat was placed in a home-built holder. The implanted neck coil was connected to the tuning and matching circuit mounted on the animal holder. During the experiment, anesthesia was maintained using a 70:30 % N_2O:O_2 mixture and 1.8 % isoflurane. Body temperature was maintained at 37 °C using a heating pad with warm water circulation. Blood gases were measured every 20 min to ensure stable physiological conditions. Cardiac pulsation and blood pressure were monitored constantly throughout the experiment.

Hyperpolarized [1-^{13}C] pyruvate solution (2.3 mL, 34.5 mM) was injected intravenously using the separator/infusion pump described in Comment et al. [12]. Injection started about 11 s after dissolution and lasted for 6 s. Three injections were performed.

2.4 MR Acquisition

All ^{13}C data were acquired on a 9.4-T, 31-cm horizontal bore magnet (Magnex Scientific, Oxford, UK) interfaced with a Varian Digital Drive console (Varian, Palo

Alto, CA, USA). The magnet was equipped with a gradient insert capable of reaching 450 mT/m in 200 μs (Resonance Research, Inc., Billerica, MA). All spectra were acquired with 32,000 complex points and spectral width of 50 kHz.

2.4.1 T_1 Measurement in In Vitro Blood Samples

The data used to obtain T_1 values for [1-^{13}C] pyruvate in blood samples at 9.4 T were acquired using an 18-mm outer diameter spherical glass bulb (Wilmad-Labglass, Buena, NJ) into which 1.5 mL of blood mixed with 0.3 mL of hyperpolarized solution was injected. Data were acquired using the radiofrequency coil assembly consisting of an inner ^{13}C linearly polarized surface coil (12 mm diameter) and a ^{1}H quadrature surface coil (two loops of 14 mm diameter) built according to a previously described design [13] and a small flip-angle pulse-acquire (4.5° at the coil center, $T_R = 1.5$ s, 160 scans) with ^{1}H WALTZ-16 decoupling [14].

2.4.2 In Vivo Measurement

The animal positioning in the magnet was checked using the above-described radiofrequency coil assembly and gradient echo images ($T_R = 60$ ms, $T_E = 3.9$ ms, matrix = 256 × 128, slice thickness = 2 mm). Spectra were acquired using the implanted neck coil and pulse-acquire sequence (90°, $T_R = 0.6$ s, 160 scans). The use of 90° pulse-angle and the fast repetition time do not lead to signal saturation because the excited blood is replaced by fresh blood during the repetition time (the coil excites ~0.0176 mL of blood which flows out of the coil in ~3.5 ms assuming the flow of 5 mL/s in arteries).

2.5 T_1 Analysis

The signal of [1-^{13}C] pyruvate at 172 ppm or [1-^{13}C] pyruvate hydrate at 180 ppm was integrated using Varian software. The T_1 relaxation times were determined by fitting the time courses of signal intensity starting at the maximum value using a two-parameter, mono-exponential decay function in Origin 8.6 (OriginLab Corporation, Northampton, MA). The decrease in total concentration and isotopic enrichment over time, measured in bench experiment under identical conditions, were used to correct the T_1 relaxation times. The pyruvate signal intensity was corrected using the slope of the linear fit of pyruvate concentration in blood versus time from 10 to 30 s (inset Fig. 3a), and using the slope of the linear fit of pyruvate enrichment in blood versus time from 10 to 20 s.

3 Results

Good quality spectra with high SNR were obtained with the radiofrequency coil implanted around the CCA in the rat after injection of hyperpolarized [1-^{13}C] pyruvate and [1-^{13}C] pyruvate hydrate mixture (Fig. 2). The SNR of the [1-^{13}C] pyruvate signal at 7.8 s without line broadening was 19 (Fig. 2). A typical, rapid,

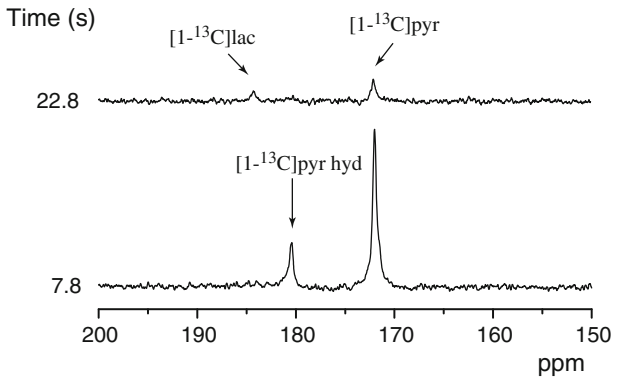

Fig. 2 Representative spectra obtained with the radiofrequency coil implanted around the CCA. **a** Spectrum obtained 7.8 s after the beginning of injection with the maximum pyruvate and pyruvate hydrate signals observed. **b** Spectrum obtained 22.8 s after the beginning of injection with the maximum lactate signal observed. Repetition time (T_R) = 0.6 s, pulse width (pw) = 120 μs, line broadening = 10 Hz

nearly linear increase of pyruvate and pyruvate hydrate signals was observed with the maximum signal at 6.0 ± 1.6 s after the beginning of injection (Fig. 3). Pyruvate and pyruvate hydrate signals then decayed as a result of T_1 relaxation, transport and metabolism. The apparent T_1s of 7.5 ± 1.3 s for pyruvate and 5.1 ± 1.1 s for pyruvate hydrate were obtained when the decay part of the time courses was fitted with the mono-exponential decay function (Table 1).

[1-^{13}C] lactate signal was also detected (Fig. 2), but the signal was too low to be fitted accurately. The highest lactate signal was about 20 times lower than the highest pyruvate signal.

In in vitro blood samples, the apparent T_1 of [1-^{13}C] pyruvate and [1-^{13}C] pyruvate hydrate was measured to be 31 ± 1 s and 23 ± 1 s, respectively. [1-^{13}C] lactate signal was observed, but the signal was about 170 times lower than pyruvate signal. The low lactate signal in in vitro blood was observed previously [15].

The concentration of pyruvate increased in blood from 0.2 mM to 1.1 mM during the first 10 s after the injection and linearly decreased to 0.2 mM in the next 20 s (bench experiments). The ^{13}C enrichment increased to 72 % at 10 s, decreased to 55 % at 20 s, and stayed constant from 20 to 50 s after the injection.

4 Discussion and Conclusions

In this work, we demonstrate that the input function of hyperpolarized [1-^{13}C] pyruvate in the rat carotid artery can be measured in vivo using an implantable neck coil. The apparent T_1 of [1-^{13}C] pyruvate was much shorter in vivo than what was observed in in vitro blood samples, 7.5 ± 1.3 s versus 31 ± 1 s, suggesting that the decrease in [1-^{13}C] pyruvate signal over time reflects not only T_1 relaxation but also a decrease in concentration and enrichment, due to transport and metabolism of

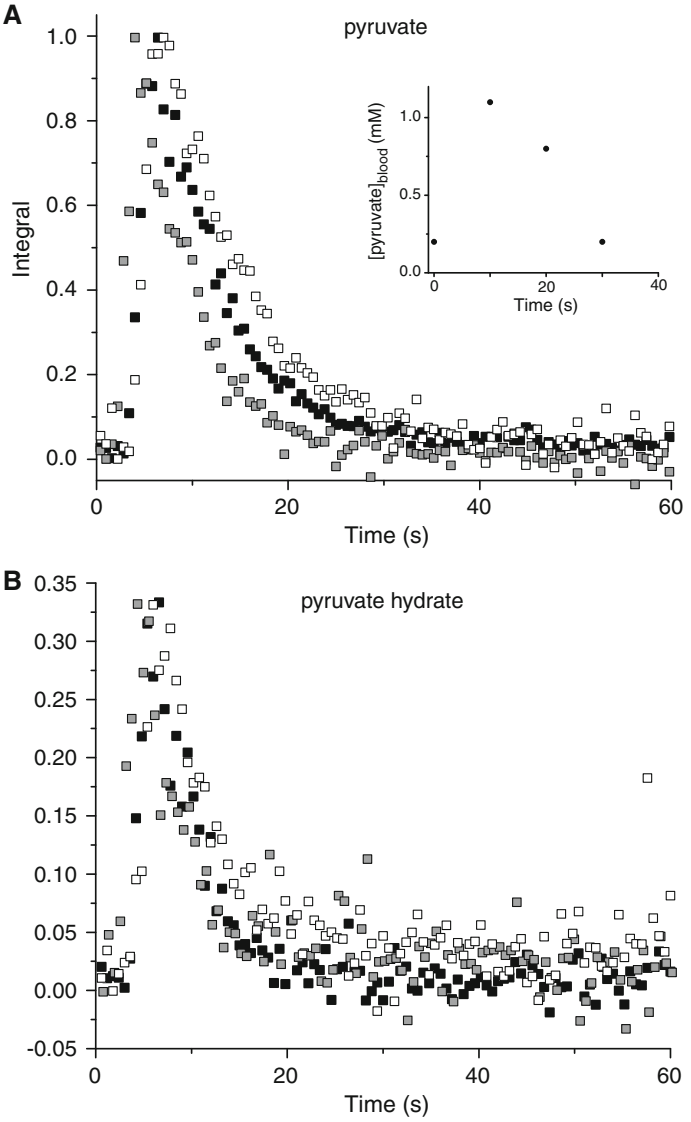

Fig. 3 Three (*black, gray*, and *open squares*) time courses of **a** pyruvate and **b** pyruvate hydrate signals obtained with the radiofrequency coil implanted around CCA after three injections of hyperpolarized [1-^{13}C] pyruvate and [1-^{13}C] pyruvate hydrate mixtures. The pyruvate time courses are shown scaled to the highest integral value in each time course. The pyruvate hydrate time courses are shown scaled to the average of the ratio of pyruvate hydrate to pyruvate of all time courses. The inset shows the change in concentration of pyruvate in the blood measured in bench experiment under identical conditions as in in vivo experiments with implantable neck coil. T_R = 0.6 s, pw = 120 μs

pyruvate in vivo. The apparent T_1 increased to 13.2 ± 4.3 s after the correction for the concentration decrease in total concentration and isotopic enrichment over time, measured separately in bench experiments under identical conditions.

Table 1 Apparent T_1 values for hyperpolarized substances measured in phantom, in vitro blood samples, and in vivo at 9.4 T

Experiment type	Dissolution solvent	pH	*n*	T_1 [1-^{13}C] pyr (s)	T_1 [1-^{13}C] pyr hyd (s)
Phantom[a]	H_2O	3	4	26 ± 9	26 ± 8
Phantom[a]	H_2O buffer	7	6	46 ± 6	37 ± 5
Phantom[a]	D_2O buffer	7	3	57 ± 8	43 ± 2
In vitro blood	H_2O buffer	7	4	31 ± 1	23 ± 1
In vivo arterial blood (uncorrected)	H_2O buffer	7	3	7.5 ± 1.3	5.1 ± 1.1
In vivo arterial blood (corrected for concentration and enrichment)	H_2O buffer	7	3	13.2 ± 4.3	

R^2 for exponential fits in in vitro blood > 0.9992

R^2 for exponential fits in in vivo arterial blood for pyr > 0.977 and pyr hyd > 0.791

n number of experiments

[a] Taken from [10]

The lactate signal observed in in vitro blood samples was very small, suggesting that the LDH activity in blood is smaller in blood in vitro than in vivo. The difference between in vitro and in vivo results might be due to higher concentration of pyruvate used in in vitro studies, different temperature (in vitro data were obtained at room temperature), denaturation of the proteins in in vitro blood, or in vivo influx of labeled lactate back into the blood after conversion from pyruvate in other organs. In vivo in blood, much higher lactate signal was observed, but the signal was still too small to use for metabolic modeling of LDH activity in the blood.

Even after correcting for the decrease in concentration and enrichment, the apparent T_1 was still significantly shorter in vivo than in vitro suggesting that additional mechanisms contribute to relaxation in vivo compared to in vitro blood experiments. Potentially, the relaxation of pyruvate could be much faster in lungs, liver, or kidneys which have high blood volume [16].

The use of the implantable coil opens up a possibility of measuring not only the input function but also the venous output function.

Acknowledgments We thank Manda Vollmers and Emily Colonna, and William Manders from Oxford Instruments Biotools for technical support. The authors thank Dr. Josef Granwehr for helpful discussions. This work was supported by the National Institutes of Health: R01 NS38672, P41 RR008079, P41 EB015894, and the W.M. Keck Foundation and by the Director, Office of Science, Office of Basis Energy Sciences, Materials Sciences and Engineering Division, of the U.S. Department of Energy under Contract No. DE-AC02-05CH11231. Funding for NMR instrumentation was provided by the Office of the Vice President for Research, the Medical School, the College of Biological Science, NIH, NSF, and the Minnesota Medical Foundation.

References

1. K. Golman, J.H. Ardenaer-Larsen, J.S. Petersson, S. Mansson, I. Leunbach, Proc. Natl. Acad. Sci. USA **100**, 10435–10439 (2003)

2. K. Golman, R. in't Zandt, M. Thaning, Proc. Natl. Acad. Sci. USA **103**, 11270–11275 (2006)
3. K. Golman, R. in't Zandt, M. Lerche, R. Pehrson, J.H. Ardenkjaer-Larsen, Cancer Res. **66**, 10855–10860 (2006)
4. A.P. Chen, M.J. Albers, C.H. Cunningham, S.J. Kohler, Y.F. Yen, R.E. Hurd, J. Tropp, R. Bok, J.M. Pauly, S.J. Nelson, J. Kurhanewicz, D.B. Vigneron, Magn. Reson. Med. **58**, 1099–1106 (2007)
5. S.E. Day, M.I. Kettunen, F.A. Gallagher, D.E. Hu, M. Lerche, J. Wolber, K. Golman, J.H. Ardenkjaer-Larsen, K.M. Brindle, Nature Med. **13**, 1521 (2007)
6. C.S. Ward, H.S. Venkatesh, M.M. Chaumeil, A.H. Brandes, M. Vancriekinge, H. Dafni, S. Sukumar, S.J. Nelson, D.B. Vigneron, J. Kurhanewicz, C.D. James, D.A. Haas-Kogan, S.M. Ronen, Cancer Res. **70**, 1296–1305 (2010)
7. K.R. Keshari, J. Kurhanewicz, R.E. Jeffries, D.M. Wilson, B.J. Dewar, M. Van Criekinge, M. Zierhut, D.B. Vigneron, J.M. Macdonald, Magn. Reson. Med. **63**, 322–329 (2010)
8. M.L. Zierhut, Y.F. Yen, A.P. Chen, R. Bok, M.J. Albers, V. Zhang, J. Tropp, I. Park, D.B. Vigneron, J. Kurhanewicz, R.E. Hurd, S.J. Nelson, J. Magn. Reson. **202**, 85–92 (2010)
9. T. Harris, G. Eliyahu, L. Frydman, H. Degani, Proc. Natl. Acad. Sci. USA **106**, 18131–18136 (2009)
10. M. Marjanska, I. Iltis, A.A. Shestov, D.K. Deelchand, C. Nelson, K. Ugurbil, P.G. Henry, J. Magn. Reson. **206**, 210–218 (2010)
11. T. Xu, D. Mayer, M. Gu, Y.F. Yen, S. Josan, J. Tropp, A. Pfefferbaum, R. Hurd, D. Spielman, NMR Biomed. **24**, 997–1005 (2011)
12. A. Comment, B. van den Brandt, K. Uffmann, F. Kurdzesau, S. Jannin, J.A. Konter, P. Hautle, W.T.H. Wenckebach, R. Gruetter, J.J. van der Klink, Concept Magn. Reson. B **31B**, 255–269 (2007)
13. G. Adriany, R. Gruetter, J. Magn. Reson. **125**, 178–184 (1997)
14. A.J. Shaka, J. Keeler, T. Frenkiel, R. Freeman, J. Magn. Reson. **52**, 335–338 (1983)
15. K.K.-C. Leung, W.W. Lam, A.P. Chen, ISMRM (Honolulu, USA, 2009), p. 2432
16. N.B. Everett, B. Simmons, E.P. Lasher, Circ. Res. **4**, 419–424 (1956)